1965ApJ...142..943S

KINEMATICS OF THE MIRA VARIABLES*

JOZEF I. SMAK† AND GEORGE W. PRESTON
Lick Observatory, University of California, Mount Hamilton
Received May 3, 1965

ABSTRACT

Radial velocities based on Lick 120-inch coudé spectrograms are given for 270 Mira variables previously unobserved for radial velocity. The great majority of these Miras have magnitudes in the interval $10 < m_{pg} < 15$. These observations are combined with those of Merrill and Feast to discuss the kinematic properties of the Miras. Distances are calculated by means of the absolute magnitudes of Osvalds and Risley and an exponential layer model of the interstellar extinction. Three values of the interstellar extinction coefficient were assumed: 1 5, 2 0, and 2.5 pg. mag kpc^{-1} Values of the Oort constant $A \sim 15$ km sec^{-1} kpc^{-1} are obtained for period groups with $P < 350$ days. A much larger value $A \sim 25$ km sec^{-1} kpc^{-1} is obtained for Miras with $P > 350$ days. The mean θ-component of the galactocentric motion for Miras decreases with increasing height above the galactic plane. This decrease is interpreted in terms of the ellipsoidal hypothesis and leads to z-dependent expressions for V_θ, A, and R_{max}, the galactocentric distance for which V_θ is a maximum.

I. INTRODUCTION

While the galactic rotation of the B-type stars and the Cepheids has been the subject of numerous studies, there are few comparable investigations for members of the disk or halo populations. It is well known that the galactic rotational velocities near the Sun of various components of these older populations are smaller than that for the very young stars. However, the lack of radial velocities for distant members of the disk and halo and the large velocity dispersions (particularly in the halo populations) have made studies of differential galactic rotation difficult or impossible. Of all the members of the older stellar populations the Miras are the most promising candidates for the study of galactic dynamics for the following reasons: (1) the studies by Merrill (1941), Merrill and Wilson (1942), and more recently, Feast (1963) show that the Miras possess a considerable spread in kinematic characteristics ordinarily used as population indicators, characteristics that are correlated, albeit imprecisely, with period; (2) the Miras are of moderately high luminosity and, more important, their spectra contain strong emission lines of H near maximum light that may be used to determine their radial velocities; (3) because of their large light ranges they have been discovered in large numbers at faint magnitudes. In this paper we present new radial-velocity data for distant Miras and a preliminary discussion of galactic motions based on all available data. Our definition of a Mira star is necessarily that of the *General Catalogue of Variable Stars* (2d ed.) from which our observing list was chosen.

II. THE OBSERVING PROGRAM

All spectrograms, except those for four stars, were obtained with the 20-inch camera of the 120-inch coudé spectrograph in the first order of a 400-groove/mm Bausch and Lomb grating (dispersion 48 Å/mm). The spectrograms for four of the stars were obtained with the air-Schmidt camera of the prime-focus spectrograph (dispersion 50 Å/mm). Kodak 103a-O emulsion was used throughout the program. It was found that in average seeing the H-emission lines of a Mira with $m_{pg} \sim$ 14–15 could be recorded in 1 hour, which was adopted as a rough limiting exposure in this first survey. A given star was observed only if its visual magnitude, estimated at the field-viewing eyepiece, was

* *Contributions from the Lick Observatory*, No. 189.

† Present address: Warsaw University Observatory, Warsaw, Poland.

© American Astronomical Society • Provided by the NASA Astrophysics Data System

1965ApJ...142..943S

less than or equal to its photographic magnitude at maximum light as given in the *General Catalogue of Variable Stars* (2d ed.). Some stars were examined several times before they became bright enough to observe. Only one spectrogram was obtained for each star. Spectrograms of one or both of the two planetary nebulae IC 418 and IC 4997 were obtained regularly with the same equipment in order to study the stability of the instrumental radial velocities and to compare the instrumental velocities to other systems. As an additional check, spectrograms of both planetaries were obtained with the 40-inch camera and two other gratings (dispersions 5.3 and 8.2 Å/mm). Finally, spectrograms (dispersion 48 Å/mm, as for the program stars) were obtained for thirteen of the Miras observed by Merrill (1941). The observing program extended over a 9-month period, March–December, 1964. Altogether, spectrograms of 270 Miras (exclusive of the thirteen observed in common with Merrill) were obtained. It might be mentioned that the rapidity with which this program was carried out with conventional equipment suggests that the days of photographic spectroscopy are not yet over. As a final aside we remark that, quite apart from those variable stars for which *no* finding charts have been published, we were unable to identify many variable stars on the basis of finding charts that exist in the literature. In our opinion it is pointless to report the discovery of variable stars that cannot be located for subsequent study. Reproductions of small portions of the Palomar Observatory Sky Survey plates or prints make excellent charts and are greatly preferable to freehand impressions of star fields.

III. MEASUREMENTS AND REDUCTIONS

With the exception of one star (DF Her; see notes to Table 3) radial velocities are based exclusively on measurements of the emission lines Hγ, Hδ, H8, and H9. Various combinations of these lines were measured depending on the quality of the exposure and the phase of the observation (which in general is not known) as tabulated below:

4 lines (Hγ, Hδ, H8, H9)	for 96 stars,
3 lines (. . . , Hδ, H8, H9)	for 21 stars,
2 lines (Hγ, Hδ, . . . , . . .)	for 127 stars,
1 line (Hγ or Hδ)	for 27 stars.

The continuous spectrum appeared at adequate density for about one-fifth of the stars observed, but because of the narrowness of the spectrograms and the inhomogeneities that might be introduced by measurement of absorption velocities in only a portion of the sample, we decided not to measure the absorption lines. The spectrograms were measured on two Gaertner long-screw (250-mm) comparators by the authors. From twenty plates measured in common, the mean difference in measured velocity (J. I. S. *minus* G. W. P.) was found to be +0.06 km/sec while the measurement error for a single line was found to be ±1.7 km/sec.

Instrumental velocities derived from the spectrograms of the planetary nebulae are based on mean velocities of the H-emission lines Hγ, Hδ, and H9 (H8 omitted due to contamination by λ 3888 He I). The mean radial velocities were found to be

IC 4997: −78.5 ± 1.2 km/sec based on 27 spectrograms (48 Å/mm),

IC 418: +56.3 ± 1.3 km/sec based on 11 spectrograms (48 Å/mm).

There is no indication that the radial velocity of either object depends on Julian date or hour angle. Single spectrograms obtained with the 40-inch camera give

IC 4997: −74.8 ± 1.0 km/sec (errors estimated from internal agreement),

IC 418: +64.0 ± 1.9 km/sec (errors estimated from internal agreement).

© American Astronomical Society • Provided by the NASA Astrophysics Data System

1965ApJ...142..943S

On the basis of the two sets of radial velocities given above and the superior definition of the 40-inch camera, we conclude that a correction of +5 km/sec should be applied to radial velocities derived from H-emission lines on the 48 Å/mm spectrograms. A similar correction of +6 km/sec is indicated by comparison with the velocity (+62 km/sec) for IC 418 given in the *General Catalogue of Stellar Radial Velocities*. However, the radial velocity for IC 4997 (−64.4 km/sec) given by Campbell and Moore (1918) differs by 14 km/sec from the average derived from our 48-Å/mm plates and by 10.4 km/sec from the velocity of our 8.2-Å/mm plate. The latter discrepancy is too large to ascribe to errors of measurement, and an examination of their original reductions shows that it is not due to errors in either the heliocentric corrections or wavelengths used by Campbell and Moore. Two 10-Å/mm spectrograms of IC 4997, ce 15536, and ce 15540, obtained with the Mount Wilson 100-inch coudé spectrograph, were kindly loaned to us by Dr. O. C. Wilson. The radial velocities from these two spectrograms, −75.2 and −74.5 km/sec, are in excellent agreement with the radial velocity from our 8-Å/mm spectrogram. Hence, while the origin of the disagreement with Campbell and Moore remains unexplained, we are sure that it is not associated with the 120-inch coudé spectrograph. On the basis of the considerations above, we consider that a correction of +4 or +5 km/sec should be applied to the radial velocities derived from the H-emission lines on 48-Å/mm spectrograms.

TABLE 1

MEAN DIFFERENCES IN VELOCITY BETWEEN H-LINES

	Hδ–H9	Hδ–H8	Hδ–Hγ
IC 4997:			
Mean value ± m e. (km/sec)	+2 6±1 8		−1 2±0 8
No. of plates	24		27
IC 418:			
Mean value ± m e (km/sec)	+0 6±1 6		+2 5±1 3
No of plates	10		11
Miras:			
Mean value ± m e. (km/sec)	−3 2±0 7	−3 2±0 6	+4.3±0 5
No. of plates	93	93	217

Systematic differences were found between velocities derived from the various H-lines of the planetary nebulae as indicated in Table 1. The differences for the Miras (also given in Table 1) are larger, of opposite sign, in the case of Hδ–H9 and, to judge from the errors, real. The absolute values of these differences may be due largely to instrumental effects, e.g., a variation of instrumental profile with wavelength. However, we tentatively attribute the difference in behavior between the planetaries and Miras to effects intrinsic in the Mira spectra, e.g., mutilation of the emission lines by overlying absorption (Joy 1947). It should be noted that the apparent run of velocity with wavelength is in reasonable agreement with that found by Merrill (1923) in his comparison of velocities derived from Hγ, Hδ, and H8 in Miras.

Since various combinations of lines were measured in different Miras as indicated above, we decided to reduce velocities derived from each line to Hδ by means of the differences for the Miras given in Table 1 before forming the average velocity for each star. Weights of 1 for H8 and H9 and 2 for Hγ and Hδ were arbitrarily adopted. Application of this procedure to the measures of the stars observed by Merrill leads to the results in Table 2. The mean difference in radial velocities is

$$\text{Merrill } \textit{minus} \text{ This study} = +1 \text{ km/sec} ,$$

which we have applied as a systematic correction to put our data on the system of Merrill. It should be noted that this correction can be reconciled with the instrumental cor-

© American Astronomical Society • Provided by the NASA Astrophysics Data System

1965ApJ...142..943S

rection derived above if it is assumed that Hγ in the Miras gives the instrumental velocity as derived from the planetary nebulae. Final quality estimates (1, 2, or 3) for each stellar radial velocity were assigned on the basis of the number of lines measured and the quality of the spectrogram. Weight 1 indicates one or two poor lines while weight 3 indicates two or more good lines.

We assumed, following Merrill, that the velocity of the star is given by the velocity derived from the absorption lines. We adopted the linear relation

$$A - E = 0.035P \text{ km/sec}, \tag{1}$$

which is based on the data in Figure 1*a* for Feast (1963). The emission velocities and absorption velocities derived from equation (1) are listed in Table 3 for 270 Miras, of which nine stars at the end of Table 3 are considered to be probable S- or C-type stars on the basis of their periods and Hβ/Hγ intensity ratios. They have been omitted in the analyses that follow, as has GV Ori, for which there is no published period.

The radial velocities contain errors due to measurement (±1–2 km/sec), dependence on phase and/or intrinsic variations in velocity (±2–3 km/sec), and dispersion in the relation between $A - E$ and P (±3–4 km/sec). Thus, we expect a random error of about ±5 km/sec for the radial velocity of a Mira for which we have a single spectrogram

TABLE 2

COMPARISON OF LICK AND MOUNT WILSON RADIAL VELOCITIES OF MIRA VARIABLE STARS

Type and Star	Measured Radial Velocity				Weighted Mean Reduced to Hδ	Merrill's Value	Merrill minus This Study
	H9	H8	Hδ	Hγ			
M:							
V And	+18 9	+ 9 4	+ 7 4	+10 3	+11	+ 8	− 3
Y And	.	. .	− 9 6	−17 2	−11	−17	− 6
UZ And	−48 5	−54 5	−56 0	−69 7	−59	−51	+ 8
U Aur	. . .	. . .	+ 8 6	0 0	+ 6	+ 7	+ 1
RV Cas	−81 2	−80 0	−86 7	−91 3	−86	−80	+ 6
R Cet			+33 8	+34 1	+36	+32	− 4
U Cet	. .	. . .	−43 4	−45 6	−42	−39	+ 3
U Cet	−32 6	−31 5	−35 6	−35 2	−34	−39	− 5
R Per	−87 8	−81 2	−86 9	−93 9	−88	−89	− 1
R Psc	.	. . .	−55 4	−62 3	−57	−59	− 2
V Tau	+62 6	+58 1	+59 7	+51 2	+57	+70*	+13*
Average ± m e.							+0 9±1 8
S:							
R And	−18 4	−25 2	−28 0	−32 6	−27	−29	− 2
R Cyg	. .	. . .	−56 4	−52 0	−52	−46	+ 6
S UMa	−16 0	−18 1	−12 8	−13 8	−14	− 4	+10
C:							
U Cyg			. .	+ 0 5	+ 5	− 7	−12
VX Gem			+47 7	+42 0	+47	+42	− 5
Other:†							
R And	−23 1	−23 5	−29 3	−28 1	−26	−29	− 3
R Aql	+28 8	+21 2	+24 0	+19 2	+23	+21	− 2
R Aql	+10 6	+13 9	+11 9	+14 7	+13	+21	+ 8
All average ± m e.							+0 5±1 5

* Merrill lists observed velocities of +70, +75, +58, and +53 for which the average is +64 If +64 is used instead of his adopted value of +70, the difference Merrill *minus* our study is reduced to +7 km/sec

† Spectrograms obtained with a calcite block in front of slit during a search for linear polarization of the emission lines.

© American Astronomical Society • Provided by the NASA Astrophysics Data System

1965ApJ...142..943S

TABLE 3

RADIAL VELOCITIES OF MIRA VARIABLE STARS

Q	Name	l^{II}	b^{II}	M_{pg} at Max.	P (days)	JD	Radial Velocity (km/sec) Em.	Abs.
2	YY And	109.8	-29.5	11.9	230.0	2438626	- 99	- 91
2	AH And	137.8	-20.0	11.0	480.2	2438626	- 27	- 10
3	AI And	107.6	-11.1	11.7	325.8	2438626	-102	- 91
3	AX And	140.5	-12.9	11.1	189.0	2438636	- 19	- 12
3	BP And	105.4	- 9.1	13.4	141.6	2438687	- 93	- 88
3	TX Aqr	48.6	-30.4	10.5	347.2	2438637	- 34	- 22
2	AV Aqr	37.2	-55.6	12.5	347.0	2438626	- 85	- 73
2	RX Aql	46.7	- 7.9	13.0	206.0	2438719	61	68
3	SS Aql	47.0	- 4.2	13.3	148.0	2438654	- 23	- 17
1	SW Aql	51.2	- 6.9	13.3	247.0	2438670	- 1	8
3	TU Aql	38.9	- 7.1	10.3	270.4	2438656	- 66	- 56
3	TV Aql	48.2	-14.9	11.4*	240.2	2438656	- 61	- 53
2	WZ Aql	47.1	-16.1	11.8	316.4	2438653	8	19
3	XY Aql	39.4	- 3.2	11.0	398.0	2438656	- 71	- 57
3	AK Aql	27.8	- 5.2	10.8	297.2	2438652	- 61	- 51
1	GK Aql	38.2	- 8.7	13.6	196.0	2438652	27	34
2	GO Aql	39.2	- 8.6	13.4	154.8	2438687	- 50	- 45
1	V 335 Aql	44.8	-19.2	11.6	177.0	2438656	3	9
2	V 386 Aql	44.1	- 6.7	12.7	334.8	2438654	22	34
1	V 397 Aql	43.4	- 8.3	13.4	183.6	2438654	66	73
3	V 430 Aql	46.3	-12.1	13.5	266.0	2438688	70	80
1	V 436 Aql	52.0	-10.4	12.5	285.0	2438654	- 31	- 21
1	V 437 Aql	53.8	- 9.3	13.5	192.0	2438656	15	22
1	V 438 Aql	48.5	-12.5	12.5	279.0	2438724	- 18	- 8
3	V 442 Aql	53.6	-11.0	12.5	308.0	2438668	- 51	- 41
3	V 456 Aql	45.3	- 7.5	13.1	350.0	2438669	2	14
3	V 466 Aql	51.4	-11.3	12.0	428.0	2438656	- 17	- 2
2	V 503 Aql	39.6	-15.7	12.5	138.2	2438654	- 92	- 87
2	V 514 Aql	38.3	-19.6	13.0	291.1	2438668	- 80	- 70
3	V 517 Aql	45.4	-16.8	12.7	305.0	2438695	12	23
1	V 530 Aql	35.1	- 7.1	12.9	366.0	2438652	14	27
2	V 540 Aql	41.9	-11.4	13.8	308.5	2438669	- 92	- 81
2	V 545 Aql	37.8	-13.8	13.5	243.5	2438669	- 91	- 83
3	V 580 Aql	37.9	-19.2	12.5	150.2	2438668	- 43	- 38
3	V 581 Aql	42.7	-16.7	12.5	215.8	2438668	40	48
1	V 592 Aql	43.6	-19.1	13.4	197.0	2438688	- 66	- 59
1	V 595 Aql	44.3	-19.6	12.5	241.3	2438668	33	42
3	V 671 Aql	39.7	-11.0	13.8	221.0	2438669	49	56
3	V 707 Aql	54.2	- 5.6	13 9	259.0	2438687	-119	-110
1	V 867 Aql	33.2	- 1.2	13.5	192.0	2438652	- 52	- 45
3	V 893 Aql	37.6	-13.9	12.0	316.7	2438687	- 54	- 43
3	Z Ari	157.0	-26.7	11.0	344.8	2438636	- 55	- 43
2	RU Ari	161.5	-41.9	11.4	353.5	2438637	20	32
3	SW Aur	169.5	-10.4	13.3	309.8	2438638	2	13
3	SZ Aur	171.1	4.6	10.2	453.4	2438652	0	16
3	VX Aur	177.6	24.0	9.6	322.2	2438653	12	24
1	VY Aur	166.8	12.8	11.8	401.8	2438656	10	24
2	AW Aur	179.5	- 1.2	12.0	695.0	2438652	- 18	6
3	AY Aur	178.4	3.6	12.0	373.6	2438638	- 30	- 16

© American Astronomical Society • Provided by the NASA Astrophysics Data System

1965ApJ...142..943S

TABLE 3 (Continued)

Q	Name	l^{II}	b^{II}	M_{pg} at Max.	P (days)	JD	Radial Velocity (km/sec) Em.	Abs.
2	BN Aur	178.9	2.9	13.6	136.0	2438719	8	13
1	BT Aur	181.3	4.0	13 0	560.0	2438687	- 18	1
3	DT Aur	173.1	- 4.5	12.5	168.8	2438638	3	9
3	GN Aur	170.9	7.5	14.0	253.0	2438652	- 47	- 38
3	GU Aur	164.1	8.5	13.1	217.0	2438653	- 35	- 27
3	SZ Cnc	210.0	26.1	10.2	315.3	2438687	- 32	- 21
1	TV Cnc	214.6	22.3	11.5	366.7	2438481	- 18	- 6
1	SU CMa	231.1	- 6.5	11.5*	248.0	2438746	- 21	- 12
1	UW CMi	218.1	12.5	13.7	340.0	2438685	2	14
3	VV CMi	216.7	15.0	11.6	334.0	2438668	66	78
3	VX CMi	218.6	14.7	11.8	272.7	2438687	40	49
1	WW CMi	211.5	6.2	13.0	178.0	2438668	74	80
3	WY CMi	212.4	7.2	13.0	274.0	2438744	35	44
2	WZ CMi	213.6	7.3	13.0	316.0	2438746	49	60
3	TX Cap	28.8	-31.6	10.9	129.4	2438724	4	9
3	RY Cet	198.6	-69.6	10.5	374.0	2438631	3	16
1	T Com	325.5	85.7	11.5	406.0	2438536	1	15
2	T Crv	298.1	45.2	11.6	401.3	2438482	- 33	- 19
3	U Crv	297.5	44.2	10.1	283.1	2438481	3	13
2	V Crv	299.2	45.2	11.7	193.6	2438481	183	189
3	ST Crv	284.0	47.7	11.7	224.6	2438577	64	72
1	RT Crt	261.6	46.2	10.8	342.7	2438483	29	41
2	AG Cyg	72.4	4.8	12.7*	296.3	2438685	-73	-62
3	AM Cyg	76.5	-6.6	11.3	370.6	2438605	-90	-77
3	AT Cyg	76.8	-8.0	11.2	263.0	2438691	26	35
2	BL Cyg	91.0	-3.6	12.9	366.0	2438605	27	39
2	BU Cyg	85.1	9.8	11.7*	157.9	2438687	-33	-27
2	CZ Cyg	75.6	-13.4	11.5*	280.0	2438605	-63	-54
2	DR Cyg	78.9	- 2.7	9.3	313.8	2438724	- 2	9
2	DV Cyg	62.8	7.2	12.5	146.7	2438688	-59	-54
1	EH Cyg	62.9	3.5	11.8	279.1	2438605	26	36
3	FM Cyg	33.8	5.6	12.3	274.0	2438631	-56	-46
3	FP Cyg	67.0	6.7	14.0	211.0	2438691	-196	-188
2	HZ Cyg	70.3	6.6	13.0	180.0	2438635	4	10
3	KM Cyg	72.3	3.2	11.4	334.7	2438656	- 32	- 20
3	LL Cyg	76.7	- 3.5	13.9	211.0	2438688	- 43	- 36
1	V 378 Cyg	75.2	-11.1	13.0	295.6	2438636	38	48
2	V 394 Cyg	83.5	8.9	11.5	417.0	2438636	- 50	- 35
2	V 419 Cyg	74.6	4.1	13.0	226.4	2438638	-187	-179
2	RW Del	55.7	-14.4	11.0	236.6	2438655	16	24
3	SZ Del	63.0	-13.8	11.0	238.2	2438655	- 12	- 3
3	TV Del	55.6	-14.6	12.7	217.0	2438656	-157	-150
2	AG Del	61.8	-12.7	10.7	238.4	2438668	- 29	- 21
3	BB Del	62.2	-18.1	11.3	240.0	2438656	41	49
3	BD Del	52.3	-15.1	13.0	262.0	2438655	- 29	- 20
2	BR Del	51.1	-23.1	10.0	337.4	2438655	- 93	- 81
1	EP Del	63.5	-13.1	12.5	430.5	2438669	43	58
3	Z Equ	59.0	-24.9	11.8	217.3	2438597	-110	-103
3	RR Equ	56.2	-26.9	10.8	269.5	2438598	- 54	- 45
1	SX Eri	205.6	-28.9	11.0*	281.6	2438654	67	77

© American Astronomical Society • Provided by the NASA Astrophysics Data System

1965ApJ...142..943S

TABLE 3 (Continued)

Q	Name	l^{II}	b^{II}	M_{pg} at Max.	P (days)	JD	Radial Velocity (km/sec) Em.	Abs.
1	TW Eri	214.6	-58.3	11.0	322.2	2438656	47	58
3	ST Gem	185.1	24.2	10.7*	246.4	2438653	- 64	- 55
3	WZ Gem	191.8	16.7	10.5	332.3	2438655	17	28
3	XY Gem	200.1	23.6	11.2	339.7	2438746	126	138
2	BC Gem	205.5	7.4	13.0	230.0	2438724	118	127
2	BR Gem	187.2	8.8	12.2	155.5	2438653	30	36
3	CE Gem	195.2	2.2	14.4	299.0	2438746	60	71
2	DO Gem	186.2	.5	14.8	213.0	2438724	- 17	- 9
1	SU Her	47.3	23.3	10.5	333.8	2438562	- 18	- 6
3	VW Her	65.8	25.1	12.0	284.8	2438691	- 8	2
3	WZ Her	44.7	19.2	12.0	247.8	2438606	- 5	4
3	XZ Her	44.9	17.1	10.3	171.7	2438566	28	34
2	AQ Her	69.4	27.8	11.1	280.1	2438483	- 8	2
1	BK Her	51.4	25.0	11.7	215.0	2438483	- 62	- 54
1	BT Her	55.2	11.4	14.0	297.0	2438598	- 27	- 16
1	CG Her	53.2	19.9	13.3	180.3	2438596	-108	-102
3	CZ Her	48.8	19.8	12.0	322.5	2438483	2	13
1	DF Her†	46.7	18.7	11.3	332.0	2438483	- 62	- 50
2	DG Her	46.6	14.1	11.1	295.0	2438574	- 87	- 77
1	DN Her	23.7	40.1	10.5	227.0	2438536	- 54	- 46
1	DO Her	41.5	40.7	10.8	216.8	2438482	- 49	- 42
3	DR Her	48.4	13.7	13.5	285.0	2438626	7	17
3	DS Her	45.4	11.1	11.0	268.0	2438596	- 65	- 56
2	DT Her	51.2	13.4	14.5	300.0	2438596	- 17	- 7
1	DU Her	47.5	11.3	15.0	270.0	2438598	-48	- 39
1	ER Her	51.4	22.9	13.0	165.0	2438577	- 42	- 36
3	EW Her	59.7	23.8	12.7	228.0	2438687	-122	-114
1	FI Her	58.0	22.0	12.4	239.0	2438575	-194	-185
3	FP Her	41.5	26.3	12.7	318.4	2438691	32	43
3	FR Her	41.8	24.3	12.0	134.2	2438483	-129	-124
1	FU Her	49.1	21.6	12.9	211.3	2438576	3	10
3	FX Her	49.6	20.3	12.5	354.0	2438694	18	30
1	GI Her	50.4	12.5	13.5	325.0	2438508	- 7	4
1	HT Her	55.6	43.2	12.6	163.2	2438536	-299	-293
2	KR Her	51.1	31.6	12.4	135.9	2438685	- 71	- 66
3	KT Her	56.6	30.1	13.5	381.0	2438638	- 51	- 38
3	KX Her	43.1	7.4	13.2	495.0	2438638	- 27	- 9
1	KZ Her	43.6	6.6	12.2	295.7	2438483	- 44	- 33
2	LO Her	43.9	5.5	13.4	471.0	2438691	31	47
1	LU Her	49.7	28.1	11.7	214.0	2438481	- 48	- 40
2	NX Her	43.8	23.0	13.5	320.0	2438508	- 27	- 16
1	348 Her	48.0	15.1	13.0	217.0	2438508	- 23	- 15
3	WW Hya	213.7	26.0	10.5	310.5	2438482	- 6	5
3	AQ Lac	96.2	- 7.2	11.7	354.5	2438652	- 35	- 23
1	AT Lac	96.3	- 8.0	12.4	171.3	2438652	-200	-194
1	BC Lac	99.4	-11.6	12.2	247.0	2438652	- 41	- 32
2	DL Lac	91.6	-10.4	12.5	375.0	2438654	3	16
3	TZ Leo	235.4	67.2	12.0	354.0	2438482	6	18
3	X Lep	218.0	-27.8	10.6	278.7	2438688	57	66
1	W Lib	350.9	30.8	11.8*	203.2	2438546	15	22

© American Astronomical Society • Provided by the NASA Astrophysics Data System

1965ApJ...142..943S

TABLE 3 (Continued)

ς	Name	l^{II}	b^{II}	M_{pg} at Max.	P (days)	JD	Radial Velocity (km/sec) Em.	Abs.
1	UU Lib	353.8	25.2	12.0	287.0	2438482	- 46	- 35
3	EE Lib	357.8	34.6	10.2	208.9	2438482	-118	-110
3	X Lyn	186.8	33.6	11.0*	321.2	2438667	- 4	7
3	RX Lyr	63.0	13.8	12.4*	248.9	2438656	-155	-146
3	SV Lyr	65.6	16.8	12.0	301.3	2438652	- 12	- 2
3	TX Lyr	68.1	23.6	11.9*	223.1	2438653	- 74	- 66
3	TY Lyr	60.1	8.7	10.3	332.2	2438655	- 36	- 25
3	YY Lyr	60.8	10.9	12.6	136.6	2438655	- 58	- 53
3	AC Lyr	57.9	8.1	13.5	181.0	2438688	- 12	- 6
3	AD Lyr	66.1	12.1	12.0	190.7	2438655	- 29	- 22
2	AS Lyr	56.5	15.1	13 1	327.0	2438653	- 44	- 32
1	BB Lyr	57.5	12.1	14.0	322.7	2438667	- 50	- 39
2	BI Lyr	59.4	11.3	12.0	249.8	2438655	60	69
2	BL Lyr	57.3	9.2	11.5	260.2	2438655	- 16	- 7
1	BM Lyr	58.8	9.5	12.7	155.0	2438655	15	21
1	BR Lyr	62.4	10.1	13 0	216.2	2438655	-147	-139
2	CK Lyr	61.2	16.4	13.0	343.0	2438653	29	41
3	DL Lyr	61.9	12.3	13.1	411.0	2438655	- 14	1
3	ER Lyr	72.2	12.2	12.0	196.6	2438724	36	43
1	FF Lyr	63.2	13.6	12.9	220.8	2438695	-109	-101
3	FP Lyr	74.0	12.3	13.0	270.0	2438653	- 27	- 18
3	HI Lyr	74.2	25.1	12.5	182.0	2438691	- 45	- 38
3	IS Lyr	59.4	18.9	13.6	281.9	2438653	- 35	- 25
3	IT Lyr	59.4	18.8	12.5	198.7	2438694	47	54
1	KZ Lyr	61.1	17.6	13.6	149.6	2438691	- 20	- 15
3	LM Lyr	68.1	19.7	13.2	326.4	2438653	- 60	- 48
1	MP Lyr	70.0	18.7	11.8	153.0	2438688	-240	-234
3	RS Mon	210.3	5.8	11.3*	263.5	2438719	- 15	- 6
3	TT Mon	221.1	4.9	8.9	323.0	2438661	50	61
3	AG Mon	217.1	2.9	11.6	155.9	2438661	50	56
3	AH Mon	217.0	3.8	11.0	374.0	2438661	122	135
3	AL Mon	220.1	2.3	12 5	243.5	2438688	83	92
1	AM Mon	222.4	1.1	12.1	432.0	2438661	4	20
3	BC Mon	224.9	12.8	10.0	272.3	2438667	- 18	- 8
1	BL Mon	209.4	5.2	13.0	144.0	2438719	43	48
3	CM Mon	209.3	3.2	13 0	150.0	2438719	20	26
3	CN Mon	214.0	.9	13.0	372.0	2438668	52	65
2	GX Mon	205.6	4.1	13.2	527.0	2438661	7	25
2	QQ Mon	206.3	3.8	13.0	222.0	2438668	83	91
1	VW Oph	27.0	20.6	10.4	284.1	2438513	-100	- 90
3	BC Oph	35.4	10.6	10.0	307.0	2438598	15	26
1	DO Oph	354.9	9.4	14.5	234.0	2438577	- 99	- 91
1	DP Oph	355.7	10.0	13.6	213.4	2438574	-149	-141
1	KT Oph	24.9	13.8	11.5	216.6	2438574	- 27	- 19
3	KU Oph	30.1	11.6	11.7	382.5	2438631	29	42
2	V 379 Oph	28.8	15.2	12.6	221.5	2438631	26	34
3	V 389 Oph	32.0	14.8	11.3	318.0	2438631	0	11
1	V 457 Oph	28.3	15.7	12.9	190.0	2438652	140	146
2	V 578 Oph	40.4	11.0	12.4	180.0	2438656	- 12	- 5
3	V 584 Oph	39.3	10.0	13.1	276.0	2438633	25	35

© American Astronomical Society • Provided by the NASA Astrophysics Data System

TABLE 3 (Continued)

Q	Name	l^{II}	b^{II}	M_{pg} at Max.	P (days)	JD	Radial Velocity (km/sec) Em.	Abs.
2	V 588 Oph	38.3	9.4	13.1	191.5	2438635	- 25	- 19
2	V 653 Oph	41.4	7.8	13.3	276.0	2438637	- 8	1
1	V 884 Oph	38.6	10.4	12.5	210.0	2438633	9	16
2	V 885 Oph	37.4	10.2	13.1	350.3	2438633	125	137
1	V 915 Oph	33.3	8.5	11.4	111.0	2438633	-35	-31
3	Y Ori	208.6	-17.4	11.5	271.3	2438655	54	64
3	RR Ori	192.9	- 2.9	10.6*	251.5	2438655	- 40	- 31
3	BK Ori	196.7	-13.9	10.3	353.7	2438719	3	15
3	CL Ori	195.9	- 9.9	11.5	215.0	2438719	- 18	- 10
3	EK Ori	201.0	- 4.6	13.3	148.0	2438655	- 13	- 8
1	EU Ori	198.2	-19.6	10.5	328.0	2438687	61	73
3	V 382 Ori	193.8	1.3	13.2	225.6	2438655	5	12
3	TZ Peg	64.8	-20.9	10.1	213.0	2438597	- 20	- 13
3	VY Peg	62.1	-39.8	12.0	377.0	2438744	14	28
3	AP Peg	69.9	-23.3	10.5	300.0	2438597	31	41
3	DG Peg	72.9	-32.1	11.0	147.8	2438688	-124	-119
3	DL Peg	101.4	-44.6	10.5	180.7	2438597	- 41	- 34
1	AL Per	144.2	- 8.9	12.6	145.0	2438635	-230	-225
3	AM Per	144.4	- 9.0	13.3	250.0	2438669	- 12	- 4
1	FG Per	151.8	- 4.8	14.0	340.0	2438635	- 41	- 29
3	GG Per	149.2	-14.0	12.0	279.4	2438635	- 63	- 54
3	S Psc	133.8	-53.4	9.7*	405.4	2438670	- 3	11
3	U Psc	134.8	-49.3	11.8*	173.4	2438631	- 41	- 35
3	RR Psc	101.1	-54.3	12.1	270.6	2438606	-135	-125
3	TZ Pup	229.1	2.3	12.0	317.0	2438687	62	73
1	UU Pup	229.4	4.2	11.8	282.0	2438687	72	82
2	UW Pup	233.4	3.2	13.0	422.0	2438687	91	106
1	FO Pup	244.7	5.6	13.3	318.0	2438688	79	90
1	Y Sge	56.2	- 4.8	13.6	146.0	2438688	- 2	3
1	RT Sge	57.9	- 7.6	12.6	299.3	2438637	13	24
2	RW Sge	56.9	- 4.1	13.0	429.0	2438626	-129	-114
1	RX Sge	57.3	- 5.1	13.0	439.0	2438637	- 3	13
2	TX Sge	58.3	- 6.2	13.5	146.3	2438694	- 4	1
3	BM Sge	58.7	- 6.5	13.5	312.0	2438670	- 8	3
1	CS Sge	59.4	- 9.4	13.0	351.0	2438641	24	36
2	AL Sgr	20.0	-13.5	10.5	78.6	2438667	- 10	- 7
3	BU Sgr	13.3	-11.5	12.0	313.0	2438667	12	23
2	W Sco	354.0	22.3	12.0*	221.4	2438546	16	23
2	X Sco	352.4	21.9	11.7*	199.9	2438546	- 66	- 59
2	V Scl	336.6	-75.0	10.2*	296.1	2438626	37	47
2	V Sct	21.7	- 4.8	12.0	254.0	2438548	23	32
3	ST Sct	21.4	- 5.9	11.5	219.5	2438483	40	48
3	RU Ser	19.4	42.8	11.6	280.0	2438633	1	11
3	WW Ser	8.6	45.0	11.4	367.5	2438602	- 4	9
3	BC Ser	12.4	38.3	10.0	238.0	2438602	46	55
1	CU Ser	9.9	11.3	13.0	263.5	2438602	- 83	- 74
3	CY Ser	13.0	8.6	11.6	289.2	2438602	0	10
2	Z Tau	192.1	- 5.4	10.7*	494.1	2438744	- 7	10
1	VX Tau	179.2	-22.2	11.3*	298.9	2438656	29	40
3	AG Tau	161.7	-19.1	12.8	208.0	2438638	16	23

© American Astronomical Society • Provided by the NASA Astrophysics Data System

1965ApJ...142..943S

TABLE 3 (Continued)

Q	Name	l^{II}	b^{II}	M_{pg} at Max.	P (days)	JD	Radial Velocity (km/sec) Em.	Abs.
3	T Tri	138.1	-26.9	11 5*	322.4	2438631	-121	-110
3	RR Vir	331.6	49.7	12.2*	217.5	2438576	- 51	- 43
2	AQ Vir	346.1	45.7	11.0	292.0	2438481	- 14	- 4
2	RW Vul	60.5	- 5.1	12.0	209.0	2438661	- 39	- 31
2	RX Vul	68.4	-13.4	11.0	457.0	2438661	- 14	2
3	SZ Vul	65.8	-10.7	12.0	253.6	2438661	-106	- 97
3	XY Vul	60.2	4.8	12.6	288.8	2438670	- 19	- 9
3	BY Vul	54.6	9.2	13.9	305.0	2438670	18	29
3	CI Vul	74.3	-13.3	12.0	317.7	2438661	- 33	- 21
2	DE Vul	61.4	- 2.9	13.8	298.0	2438670	3	14
				C- or S-TYPE MIRAS				
1	SU Aql	41.7	- 8.0	12.4	393.0	2438654	39	53
3	QU Aql	47.1	- 8.3	13 5	607.0	2438669	12	33
2	IW Cas	114.7	-13.4	11.5	383.6	2438653	- 33	- 19
2	FF Cyg	78.1	- 2.1	9.7*	323.9	2438656	5	16
2	RT Gem	195.7	7.3	11.0	350.4	2438667	105	118
2	VX Gem	202.2	11.2	10.8	377.9	2438653	48	61
3	AO Gem	189.8	26.8	12.1	311.6	2438746	- 17	- 6
2	SZ Lac	103.3	- 6.0	12.8	332.5	2438652	- 74	- 62
3	BD Mon	226.1	12.7	11.8*	366.0	2438688	45	58
				STAR WITH NO PUBLISHED PERIOD				
3	GV Ori	189.5	-11.9	13.0		2438719	47	

* An estimated color index of + 1.5 mag. has been added to the visual magnitude if only the latt is given in the General Catalogue of Variable Stars.

† The radial velocity is derived from the emission lines λ4202 and λ4308 of Fe I.

© American Astronomical Society • Provided by the NASA Astrophysics Data System

1965ApJ...142..943S

of average quality. This estimate compares favorably with the mean error calculated for a single spectrogram in Table 2 on the assumption that Merrill's velocities are error-free. Finally, in view of the uncertainty of our mean difference, Merrill *minus* this study (see Table 2), we cannot rule out the possibility of a systematic error of the order of 2 km/sec in our radial velocities.

IV. DISTANCES

Since the great majority of magnitudes given in the *General Catalogue of Variable Stars* are photographic, we corrected all visual magnitudes to the photographic scale by addition of $B - V = +1.5$ obtained from Smak (1964). The visual magnitudes refer almost exclusively to stars brighter than $m_v = 10$ for which interstellar reddening corrections to $B - V$ may be neglected relative to other errors. Next we adopted a smooth relation between absolute photographic magnitude and period based on the results of Osvalds and Risley (1961) as follows:

$$\begin{aligned} M_{pg} &= -0.2\,, & P &< 140 \text{ days}\,; \\ M_{pg} &= -13.4 + 5.4 \log P\,, & P &> 140 \text{ days}\,. \end{aligned} \tag{2}$$

The cut-off point at 140 days is arbitrary. Osvalds and Risley and Feast used 149 days. However, our data contain a higher proportion of high-velocity stars in the interval $140 < P < 150$ than is found in their samples. We assume that high velocity is indicative of high luminosity.

In general there are no color excesses known for faint Miras and in any event recent reports by Johnson (1965) support arguments that the ratio of total to selective absorption is not constant in all directions and in all parts of the Galaxy. Therefore, we have resorted to a simple exponential layer model for the interstellar medium of the form employed by Parenago (1945) for which

$$A_{pg} = \frac{a_0 \beta}{\sin b}\left[1 - \exp\left(\frac{-r \sin b}{\beta}\right)\right]. \tag{3}$$

We adopted $\beta = 150$ pc as a compromise between the value 125 pc given by Zonn (1956) and a more recent determination of 187 pc by Abt and Golson (1962). We then computed distances for our stars as well as those of Merrill and Feast with equations (2) and (3) by means of an iterative routine devised for the Observatory's IBM 1620 computer for a series of values of a_0 ($=1.5$, 2.0, and 2.5 mag/kpc) that should bracket the appropriate average value for stars chosen by apparent magnitude (rather than true distance) as we have done. The distribution of our stars projected on the galactic plane is shown in Figure 1 for $a_0 = 2.0$.

V. ANALYSIS OF THE RADIAL VELOCITIES

The analyses that follow are based on the radial velocities of the M-type Miras published by Merrill, by Feast, and those listed in Table 3 of this paper. We first reduced our absorption velocities, V_r, to the local standard of rest used by Feast and defined by

$$\begin{aligned} u_0 &= +10.11 \text{ toward } l^{II} = 0^0\,, & b^{II} &= 0\,, \\ v_0 &= +\ 9.63 \text{ toward } l^{II} = 90^0\,, & b^{II} &= 0\,, \\ w_0 &= +\ 6.25 \text{ toward } b^{II} = +90^0\,. \end{aligned}$$

We denote the reduced velocities by V_r'. The superscript "II" for l and b has been omitted everywhere below. These velocities are the equivalents of the values of ρ given by Feast for his stars and those of Merrill. The stars were then divided into groups according to period, galactocentric distance R, and distance from the plane z as indicated

© American Astronomical Society • Provided by the NASA Astrophysics Data System

1965ApJ...142..943S

in Table 4. For each group the average components of motion V_R, V_θ, and V_z in the cylindrical coordinate system R, θ, z were determined by least-squares solutions of the equation

$$V_r' + V_c \sin l \cos b = V_R \cos a \cos b + V_\theta \sin a \cos b + V_z \sin b \,, \qquad (4)$$

where $\sin a = (R_0/R) \sin l$, and where it is assumed that V_c, the circular velocity of the local standard of rest, is 250 km/sec and the distance from the Sun to the galactic center $R_0 = 10$ kpc. Note that $V_R = -(dR/dt)$. The reason for omitting a K-term in equation (4) is discussed in § VI*a*. In addition, velocity dispersions σ_R, σ_θ, σ_z where computed from least-squares solutions of

$$\sigma_R^2(\cos a \cos b)^2 + \sigma_\theta^2(\sin a \cos b)^2 + \sigma_z^2 \sin^2 b = (\Delta V_r')^2 \,, \qquad (5)$$

where

$$\Delta V_r' = V_r' + V_c \sin l \cos b - V_R \cos a \cos b - V_\theta \sin a \cos b - V_z \sin b \,. \qquad (6)$$

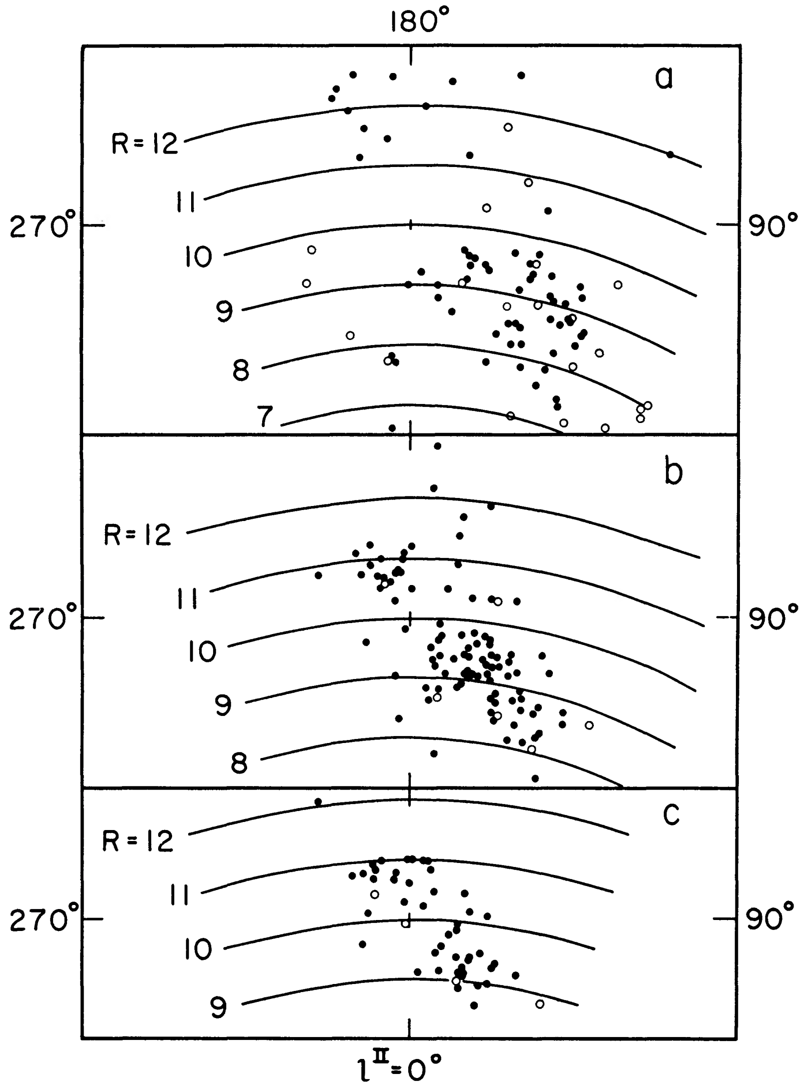

FIG. 1.—Distributions projected on the galactic plane for Mira variable observed in this study. (*a*) $140 < P < 240$ days; (*b*) $240 < P < 340$ days; (*c*) $340 < P < 700$ days. Filled and open circles denote stars with $|z| < 1$ kpc and $|z| > 1$ kpc, respectively.

© American Astronomical Society • Provided by the NASA Astrophysics Data System

1965ApJ...142..943S

Results of these solutions are given in Table 5. Because of the spatial distributions of the stars in the various groups of Table 4 (see Fig. 1), it was usually not possible to obtain accurate values of the velocity dispersions in all three coordinates for any one group. In several cases we obtained negative squares of the dispersions. These cases are indicated by the abbreviation "imag." in Table 5. In several cases the values of V_R and V_z are comparable to or exceed their dispersions in Table 5. In such cases the calculated dispersions would have been larger if we had set V_R and V_z equal to zero, the values we expect from the study of Feast. His stars were distributed more uniformly over the sky than those in a number of our groups and therefore are more suitable for a study of the motions in the R and z directions (see Fig. 1). In most instances his estimates of σ_R and σ_z are of much greater accuracy than ours.

TABLE 4

GROUPS USED TO ESTIMATE V_R, V_θ, V_z AND VELOCITY DISPERSIONS FROM EQUATIONS (4) AND (5)

GROUP	INTERVALS OF			a_0=1 5			a_0=2 0			a_0=2 5		
	P (Days)	R (kpc)	z (kpc)	$\langle P \rangle$	$\langle R \rangle$	No of Stars	$\langle P \rangle$	$\langle R \rangle$	No of Stars	$\langle P \rangle$	$\langle R \rangle$	No of Stars
1	140–240	7 0– 8 0	<1	202	7 53	10	199	7 71	12	196	7 67	8
2	140–240	8 0– 9 0	<1	192	8 51	34	192	8 61	32	195	8 62	35
3	140–240	9 0–10 0	<1	202	9 45	52	201	9 46	60	201	9 46	65
4	140–240	10 0–11 0	<1	197	10 42	21	198	10 40	22	195	10 39	23
5	140–240	11 0–13 0	<1	182	12 05	19	177	11 84	20	179	11 59	19
6	140–240	7 0–10 0	>1	198	8 83	37	194	8 75	33	192	8 86	30
7	240–340	8 0– 9 0	<1	285	8 59	28	285	8 65	26	283	8 65	25
8	240–340	9 0–10 0	<1	290	9 49	122	290	9 51	127	290	9 52	135
9	240–340	10 0–11 0	<1	299	10 47	66	300	10 47	74	299	10 46	78
10	240–340	11 0–13 0	<1	294	11 39	23	281	11 44	17	281	11 36	14
11	340–700	8 0– 9 5	<1	392	9 19	33	395	9 23	28	394	9 28	27
12	340–700	9 5–10 5	<1	404	9 96	83	406	9 97	90	404	9 97	98
13 . .	340–700	10 5–12 0	<1	425	10 79	24	420	10 83	20	414	10 83	19

We also computed the slope (A) and the curvature (α) of the rotation-curves for various period groups from least-squares solutions of

$$V_r' + V_c \sin l \cos b = U \cos l \cos b + V \sin l \cos b + W \sin b$$
$$- 2A(R - R_0) \sin l \cos b - 2\alpha(R - R_0)^2 \sin l \cos b \,, \qquad (7)$$

where U, V, and W are the rectangular components of the galactocentric group motion at $R = R_0$,

$$A = -\tfrac{1}{2}R_0 \frac{d\omega(R)}{dR}\bigg|_{R=R_0}, \qquad \alpha = -\tfrac{1}{4}R_0 \frac{d^2\omega(R)}{dR^2}\bigg|_{R=R_0} \qquad (8)$$

and

$$\omega(R) = \frac{V_\theta(R)}{R}. \qquad (9)$$

The notation employed is that of Kraft and Schmidt (1963). Two cases were considered. In the first A and α were both determined. In the second we assumed that $\alpha = 0$. Finally, solutions of equations (4), (5), and (7) were made for values of R based on equations (2) and (3) and for the three assumed values of $a_0 = 1.5$, 2.0, and 2.5. The results, all calculated with the IBM 1620 computer, are summarized in Table 6.

© American Astronomical Society • Provided by the NASA Astrophysics Data System

1965ApJ...142..943S

TABLE 5

SOLUTIONS FOR V_R, V_θ, V_z AND σ_R, σ_θ, σ_z WITH a_o = 1.5, 2 0, AND 2 5

a_o = 1 5

Group	P	⟨R⟩	⟨z⟩	V_R	V_θ	V_z	σ_R	σ_θ	σ_z
1	140 - 240	7 53	<1	18 ± 12	229 ± 14	-85 ± 33	6 ± 72	24 ± 7	59 ± 63
2	140 - 240	8 51	<1	10 ± 21	199 ± 21	- 5 ± 51	46 ± 64	23 ± 97	243 ± 56
3	140 - 240	9.45	<1	-2 ± 19	194 ± 11	-10 ± 22	imag.	79 ± 10	11 ± 194
4	140 - 240	10 42	<1	50 ± 27	176 ± 20	- 6 ± 25	44 ± 42	62 ± 17	53 ± 26
5	140 - 240	12 05	<1	6 ± 9	213 ± 24	24 ± 58	26 ± 10	imag.	156 ± 39
6	140 - 240	8.83	>1	26 ± 33	127 ± 19	- 9 ± 21	imag.	85 ± 17	79 ± 27
7	240 - 340	8 59	<1	21 ± 15	213 ± 12	-21 ± 25	25 ± 24	40 ± 8	11 ± 192
8	240 - 340	9 49	<1	-10 ± 7	228 ± 5	- 1 ± 9	45 ± 7	46 ± 4	23 ± 19
9	240 - 340	10 47	<1	3 ± 8	223 ± 8	- 9 ± 12	55 ± 7	32 ± 12	35 ± 18
10	240 - 340	11 39	<1	1 ± 11	181 ± 25	14 ± 28	40 ± 14	imag.	64 ± 40
11	340 - 700	9 19	<1	-12 ± 13	269 ± 16	9 ± 35	55 ± 14	48 ± 16	imag.
12	340 - 700	9.96	<1	- 5 ± 5	240 ± 4	3 ± 5	36 ± 4	21 ± 4	22 ± 7
13	340 - 700	10.79	<1	4 ± 7	207 ± 18	-25 ± 28	23 ± 10	58 ± 13	imag.

a_o = 2 0

Group	P	⟨R⟩	⟨z⟩	V_R	V_θ	V_z	σ_R	σ_θ	σ_z
1	140 - 240	7.71	<1	33 ± 20	211 ± 26	-22 ± 57	imag.	50 ± 18	145 ± 111
2	140 - 240	8 61	<1	- 3 ± 15	221 ± 16	-51 ± 40	42 ± 30	34 ± 31	155 ± 49
3	140 - 240	9 46	<1	18 ± 21	178 ± 13	- 5 ± 25	90 ± 30	76 ± 15	55 ± 58
4	140 - 240	10 40	<1	37 ± 26	171 ± 20	- 2 ± 25	63 ± 26	59 ± 18	48 ± 29
5	140 - 240	11.84	<1	- 3 ± 13	193 ± 34	46 ± 89	37 ± 30	60 ± 54	195 ± 155
6	140 - 240	8 75	>1	27 ± 37	143 ± 22	0 ± 23	78 ± 57	89 ± 23	65 ± 41
7	240 - 340	8.65	<1	7 ± 20	216 ± 17	- 7 ± 31	34 ± 21	49 ± 9	imag.
8	240 - 340	9 51	<1	- 8 ± 7	229 ± 5	0 ± 8	45 ± 6	46 ± 4	24 ± 18
9	240 - 340	10.47	<1	2 ± 8	219 ± 8	- 4 ± 11	58 ± 6	30 ± 13	40 ± 15
10	240 - 340	11 44	<1	4 ± 8	186 ± 21	-34 ± 24	26 ± 9	imag.	61 ± 20
11	340 - 700	9.23	<1	-12 ± 14	271 ± 18	12 ± 39	58 ± 14	47 ± 20	imag.
12	340 - 700	9.97	<1	- 2 ± 5	242 ± 4	2 ± 5	35 ± 4	25 ± 4	21 ± 7
13	340 - 700	10.83	<1	- 1 ± 9	194 ± 21	-31 ± 30	21 ± 13	63 ± 14	imag.

a_o = 2.5

Group	P	⟨R⟩	⟨z⟩	V_R	V_θ	V_z	σ_R	σ_θ	σ_z
1	140 - 240	7 67	<1	5 ± 49	269 ± 71	120 ± 152	146 ± 17	imag.	imag.
2	140 - 240	8.62	<1	10 ± 15	225 ± 16	-43 ± 38	14 ± 98	37 ± 28	181 ± 56
3	140 - 240	9.46	<1	0 ± 19	181 ± 13	-13 ± 24	84 ± 30	76 ± 16	68 ± 50
4	140 - 240	10.39	<1	40 ± 25	175 ± 19	- 3 ± 25	61 ± 26	58 ± 17	49 ± 28
5	140 - 240	11 59	<1	-7 ± 13	170 ± 35	60 ± 89	29 ± 34	67 ± 49	226 ± 117
6	140 - 240	8.86	>1	6 ± 34	137 ± 21	- 2 ± 21	imag.	73 ± 27	84 ± 29
7	240 - 340	8.65	<1	-1 ± 20	236 ± 17	12 ± 31	52 ± 12	35 ± 11	imag.
8	240 - 340	9 52	<1	-7 ± 6	227 ± 5	1 ± 8	44 ± 6	47 ± 4	21 ± 19
9	240 - 340	10 46	<1	4 ± 8	217 ± 8	- 5 ± 11	55 ± 6	33 ± 12	38 ± 16
10	240 - 340	11.36	<1	0 ± 10	164 ± 26	-74 ± 29	14 ± 22	37 ± 35	68 ± 19
11	340 - 700	9 28	<1	-11 ± 15	277 ± 19	9 ± 39	60 ± 15	46 ± 23	imag.
12	340 - 700	9 97	<1	-1 ± 5	241 ± 4	4 ± 5	32 ± 4	25 ± 4	24 ± 6
13	340 - 700	10.83	<1	-2 ± 10	196 ± 22	-37 ± 32	24 ± 13	64 ± 15	imag.

© American Astronomical Society • Provided by the NASA Astrophysics Data System

1965ApJ...142..943S

TABLE 6

SOLUTIONS FOR U, V, W, A, AND α WITH a_o = 1.5, 2.0, AND 2.5

P	z	N	U	V	W	A	α
			a_o = 1.5				
140 - 240	<1	141	-4 ± 8 -2 ± 8	186 ± 11 192 ± 9	-11 ± 15 -14 ± 15	16.3 ± 4.0 16.4 ± 4.0	- 2.3 ± 2.0
140 - 240	>1	53	26 ± 23 19 ± 24	142 ± 23 147 ± 24	- 3 ± 18 -11 ± 18	-11.8 ± 12.5 +4.2 ± 9.8	- 8.5 ± 4 3
240 - 340	<1	243	-6 ± 5 -7 ± 5	228 ± 5 225 ± 5	- 3 ± 7 - 2 ± 7	14.3 ± 3.1 13 3 ± 3.0	+ 3.0 ± 2.4
340 - 700	<1	142	-9 ± 5 -5 ± 5	236 ± 5 243 ± 5	+ 3 ± 6 + 3 ± 7	25.8 ± 4 6 22.6 ± 4.6	-12.0 ± 3.7
			a_o = 2.0				
140 - 240	<1	148	0 ± 9 1 ± 9	180 ± 11 186 ± 10	-14 ± 16 -17 ± 15	17.0 ± 4.9 17.6 ± 4.9	- 3.1 ± 3.1
140 - 240	>1	46	7 ± 26 0 ± 27	157 ± 25 164 ± 26	+ 4 ± 19 - 2 ± 19	-8.7 ± 14.0 +6.1 ± 10.8	- 8.3 ± 5.2
240 - 340	<1	246	-5 ± 5 -6 ± 5	228 ± 5 225 ± 5	- 3 ± 7 - 2 ± 7	16.1 ± 3.6 14.2 ± 3.4	+ 5.1 ± 3.1
340 - 700	<1	142	-9 ± 5 -5 ± 5	236 ± 5 242 ± 5	+ 3 ± 6 + 3 ± 7	28.4 ± 5.1 25.5 ± 5.2	+15.8 ± 5.0
			a_o = 2.5				
140 - 240	<1	151	0 ± 9 +2 ± 9	176 ± 11 184 ± 10	-13 ± 16 -17 ± 16	19 5 ± 5.9 21.6 ± 5.7	- 6.2 ± 4.2
140 - 240	>1	43	-3 ± 24 -7 ± 24	161 ± 24 166 ± 24	+ 1 ± 17 - 2 ± 17	-8.5 ± 13.7 +1.1 ± 10.3	- 6.0 ± 5.8
240 - 340	<1	254	-3 ± 5 -5 ± 5	228 ± 5 224 ± 5	- 2 ± 6 - 1 ± 6	18 6 ± 3.9 14.8 ± 3.6	+ 7.3 ± 3.4
340 - 700	<1	144	-9 ± 5 -6 ± 5	236 ± 5 243 ± 5	+ 4 ± 6 + 3 ± 7	31.5 ± 5.6 28.7 ± 5.8	-20 6 ± 6.6

© American Astronomical Society • Provided by the NASA Astrophysics Data System

1965ApJ...142..943S

VI. DISCUSSION

a) General Remarks

Our results may be conveniently examined in Figure 2, which contains plots of $\omega(R) = V_\theta/\langle R\rangle$ versus R for one value of a_0, and in Figure 3 which shows the variation of $V(=V_\theta$ at $R = 10)$ and A with period. The values of V increase with period as found

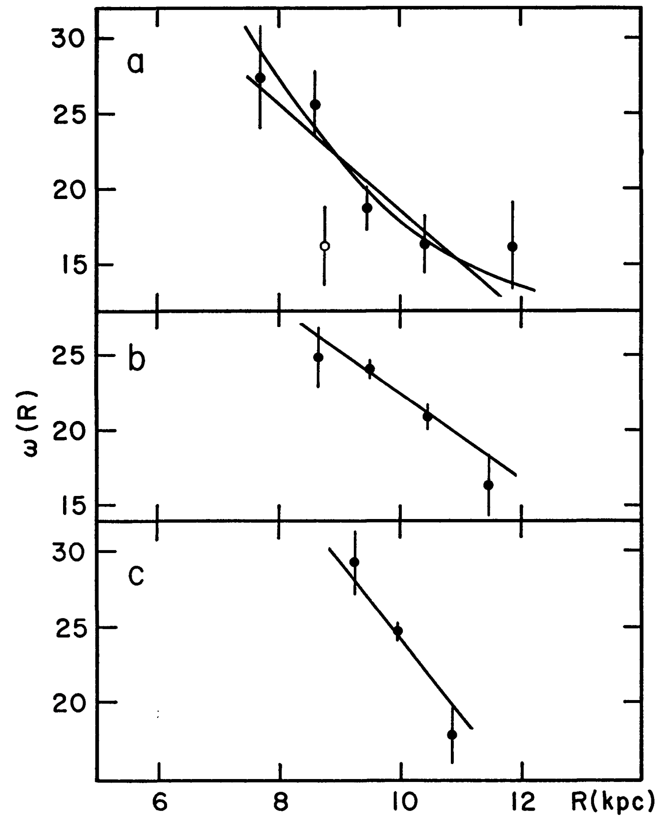

FIG. 2.—The variation of $\omega(R) = V_\theta/\langle R\rangle$ versus R for the case $a_0 = 2\ 0$ mag kpc^{-1} and for stars with (*a*) $140 < P < 240$ days; (*b*) $240 < P < 340$ days; (*c*) $340 < P < 700$ days. The straight lines denote solutions in Table 6 for which $\alpha = 0$. The curve line in (*a*) refers to the solution for both A and α. The open circle in (*a*) denotes a value of V_θ for stars with $|z| > 1$. The vertical bars denote the probable errors of the determinations.

by Merrill and by Feast. The values of V are not very sensitive to the inclusion or exclusion of the α-term in equation (7), and the average values of U and W are satisfactorily small in all cases. The values of A are not sensitive to this choice and exceed their probable errors by comfortable margins for all the groups for which $z < 1$. A comparison of our errors with those of Feast, who first looked for the effects of differential galactic rotation in the Mira radial velocities, indicates the need for radial velocities for stars at distances greater than 1 kpc if A is to be estimated with any precision. For the first (shortest) two period groups the values of $A \sim 15$ are surprisingly similar to those obtained for the B-type stars (Rubin and Burley 1964) and the Cepheids (Kraft and Schmidt 1963). However, the values for the group with $340 < P < 700$ exceeds the maximum possible value of about 18 km/sec/kpc for point mass attraction with $V_c = 250$ km/sec and $R_0 = 10$ kpc. We can only suspect that the distances for this group have been underestimated. In order to obtain values of $A \sim 15$ the distances would have to be

© American Astronomical Society • Provided by the NASA Astrophysics Data System

1965ApJ...142..943S

increased systematically by a factor of about 1.7. Errors in the assigned distances might arise in several ways:

1. The luminosities may have been underestimated. In this case the absolute magnitudes would have to be decreased by more than 1 magnitude. Such a correction is incompatible with the errors (~10 per cent) in the mean parallaxes quoted by Osvalds and Risley.

2. There may be a selection effect present in our data due to dispersion in absolute magnitude. If such dispersion exists, then for stars selected by apparent magnitude the

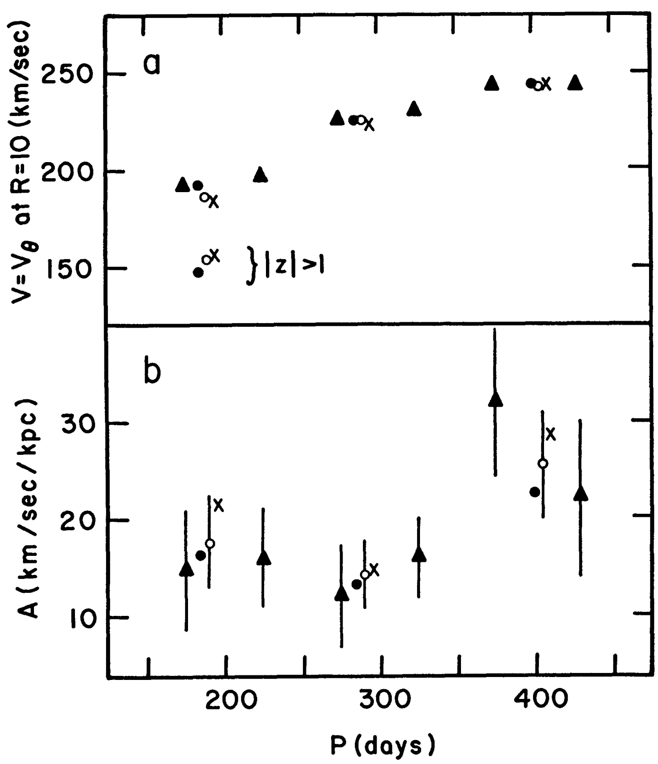

FIG. 3.—(*a*) The variation of V with period. Coding is as follows: filled circles, open circles, and crosses denote values of V in Table 6 for which $a_0 = 1.5$, 2.0, and 2.5, respectively. Triangles denote values of V for the smaller period intervals in Table 7 with $a_0 = 1.5$. (*b*) The variations of A with period. Coding is as in Fig. 3, *a*. Vertical bars denote probable errors.

absolute magnitudes will be brighter than the mean for the class by an amount $\Delta M \sim -\frac{1}{4}\sigma_M^2$, where σ_M is the dispersion in absolute magnitude (Stromberg 1936). For the required correction of -1.0 to -1.5 mag. (the precise value depends on the correct value of a_0), the value of σ_M would have to be between ± 2 and ± 3 mag. In this connection it should be noted that Feast's spectroscopic absolute magnitudes indicate a dispersion of this order *at all periods*. His dispersions are, if anything, larger at shorter periods.

3. The adopted values of a_0 may be too large. However, this cannot be the whole source of the difficulty since the average value of A_{pg} for the case where $a_0 = 1.5$ is only about 0.5 mag. for the $340 < P < 700$ group.

4. The apparent magnitudes in the *General Catalogue of Variable Stars* may be systematically in error. In this regard we would have to suspect the distance scales for all period groups, i.e., such errors cannot be responsible for the difference in values of A in the various period groups. A discussion of errors in apparent magnitudes is beyond the

© American Astronomical Society • Provided by the NASA Astrophysics Data System

1965ApJ...142..943S

scope of this paper. It suffices to say that a homogeneous set of apparent magnitudes at maximum light for faint Miras is urgently needed.

To summarize, several possible sources of error may be present in a variety of combinations in our distances. While these errors may be present in all three period groups, the steep increase in A between the second and third groups suggests that the errors are peculiar to the Miras with periods greater than about 350 days. This notion is supported by the data in Table 7 and Figure 3 (which contains solutions for six period groups rather than three). The steep increase in A near 350 days persists when the period intervals of the groups are halved. The results of Feast's analysis are also given in Table 7. Although he did not stress the fact, his data also indicate an increase in A near $P = 350$ days. Finally it should be noted that, because of the longitude distribution of the Miras

TABLE 7

COMPARISON OF SOLUTIONS FOR U, V, W, AND A OF FEAST AND OF THIS STUDY*

	P	N	U	V†	W	A
All data	140–200	68	-1 ± 15	194 ± 15	-30 ± 29	$+15\pm6$
Feast Group II	149–200	41	-33 ± 23	140 ± 25	$+7\pm27$	-12 ± 17
All data	200–250	94	-1 ± 9	196 ± 11	-12 ± 15	$+16\pm5$
Feast Group III	200–250	70	$+10\pm11$	199 ± 10	-5 ± 10	$+8\pm7$
All data	250–300	112	-9 ± 7	225 ± 8	0 ± 10	$+12\pm5$
Feast Group IV	250–300	73	-2 ± 10	227 ± 10	$+4\pm10$	$+2\pm8$
All data	300–350	127	-4 ± 6	230 ± 5	$+5\pm8$	$+16\pm4$
Feast Group V	300–350	80	-2 ± 7	228 ± 6	$+6\pm8$	$+17\pm9$
All data	350–400	59	-4 ± 8	242 ± 9	$+5\pm10$	$+32\pm8$
Feast Group VI	350–410	54	-3 ± 7	237 ± 8	-1 ± 8	$+24\pm13$
All data	400–700	66	-11 ± 7	241 ± 7	-14 ± 12	$+22\pm8$
Feast Group VII	>410	33	-16 ± 9	244 ± 8	$+10\pm18$	. .

* Solutions for "All data" assume a_0 = 1 5

† The values for Feast's groups are derived from Feast's data on the assumption that V_c = 250 km/sec

with distances greater than 1 kpc (mostly Lick observations), a systematic error in velocities of instrumental origin will enter the values of A roughly as the systematic error divided by the mean distance of the stars. On the basis of the discussion in § III we expect such errors to be of the order of ± 1 km sec^{-1} kpc^{-1}. Furthermore, the longitude distribution of the distant Miras (see Fig. 1) makes it unfeasible to attempt to eliminate such errors by the inclusion of a K-term in equation (7).

The values of a for all period groups are poorly determined. We believe that this is due to the fact that in general σ_θ is large compared with the derivatives of V_θ involved in the calculation of a while the numbers of stars at large distances, which largely control the values of a, are small (see Table 4). The number of radial velocities for distant stars will have to be doubled or tripled before curvature of the galactic rotation-curves for the Miras can be determined satisfactorily. It may be noted (see Table 6) that the calculated values of A are not critically dependent on the inclusion or exclusion of the a-term except in the case of the group with $140 < P < 240$ and $|z| > 1$ for which the values of A are indeterminate in either case. It should also be noted that for the group with $340 < P < 700$ the inordinately large values of a suggest an error in the distance scale in the same sense as that indicated by values of A.

© American Astronomical Society • Provided by the NASA Astrophysics Data System

1965ApJ...142..943S

b) The Variation of V_θ with z

The solutions by Feast and by us give values of V and A that agree to within their probable errors for all groups except the first with $P < 200$ days (see Table 7). In that case the values of both V and A differ by more than the sum of the errors of their respective determinations. An explanation for this discrepancy appears to lie in the fact that our solution refers to stars within 1 kpc of the galactic plane while Feast's analysis includes stars at all z-distances. The data in Table 8 demonstrate that only for the shortest periods does the restriction on z alter the sample significantly. The effect of this restriction is apparent in Tables 5 and 6 and in Figures 2 and 3, where it can be seen that for $140 < P < 240$ the value of V_θ for $|z| > 1$ is smaller by $\sim$70 km/sec than that for $|z| < 1$ at $R = 8.8$ kpc and smaller by $\sim$30 km/sec at $R = 10$. While the errors of the determinations of V_θ are large for $|z| > 1$, it appears safe to conclude that V_θ decreases with height above the plane.

We explore some consequences of this conclusion. Oort (1928) showed that, if an ellipsoidal distribution of stellar velocities is to satisfy the equation of continuity in a

TABLE 8

AVERAGE VALUES OF z FOR THREE PERIOD GROUPS AND TWO ASSUMED VALUES OF a_0

P (Days)	$a_0 = 1\ 5$					$a_0 = 2\ 0$				
	$\|z\|<1$		$\|z\|>1$		All z	$\|z\|<1$		$\|z\|>1$		All z
	$\langle\|z\|\rangle$	N	$\langle\|z\|\rangle$	N	$\langle\|z\|\rangle$	$\langle\|z\|\rangle$	N	$\langle\|z\|\rangle$	N	z
140–240	0 47	138	1 60	52	0 78	0 44	146	1 60	44	0 71
240–340	39	242	1 35	28	49					.
340–700	0 25	142	1 46	6	0 30					

region of the Galaxy, then the velocity dispersions $h = 1/\sqrt{(2)}\sigma_R$ and $k = 1/\sqrt{(2)}\sigma_\theta$ and the mean velocity of rotation V_θ are related to the coordinates by

$$h^2 = c_1 + c_5 z^2 , \tag{10}$$

$$k^2 = c_1 + c_2 R^2 + c_5 z^2 , \tag{11}$$

and

$$V_\theta = \frac{c_3 R}{c_1 + c_2 R^2 + c_5 z^2} , \tag{12}$$

where $c_1, \ldots, c_5$ are constants. If, for a given value of $R = R'$ we know V_θ for two values of z, we can evaluate the quantities

$$M = \frac{c_3}{c_5} R' = \frac{V_{\theta 1} V_{\theta 2} (z_1^2 - z_2^2)}{V_{\theta 2} - V_{\theta 1}} \tag{13}$$

and

$$N = \frac{c_1 + c_2 R'^2}{c_5} = \frac{V_{\theta 1} z_1^2 - V_{\theta 2} z_2^2}{V_{\theta 2} - V_{\theta 1}} , \tag{14}$$

which, together with the ratio h/k at $(R = R_0, z = 0)$,

$$L_0 = \frac{h_0}{k_0} = \frac{c_1}{c_1 + c_2 R_0^2} , \tag{15}$$

© American Astronomical Society • Provided by the NASA Astrophysics Data System

1965ApJ...142..943S

may be used to determine the constants

$$c_1 = k_0^2 L_0^2\,, \quad c_2 = k_0^2 \frac{(1-L_0^2)}{R_0^2}\,, \quad c_3 = k_0^2 \frac{M}{NR'}\left[L_0^2 + (1-L_0^2)\left(\frac{R'}{R_0}\right)^2\right], \text{ and}$$
$$c_5 = k_0^2 \frac{1}{N}\left[L_0^2 + (1-L_0^2)\left(\frac{R'}{R_0}\right)^2\right]. \tag{16}$$

Relevant values of V_θ and z at two values of R for the group with $140 < P < 240$ are taken from Tables 5 and 6 and the resulting values of M and N are collected in Table 9. If these values of M and N are substituted into equation (16) and thence into equation (12) we find that the observed variation of V_θ with R at $z = 0.45$ is reproduced only if

TABLE 9

SUMMARY OF DATA AND CALCULATIONS USED TO DERIVE V_θ (R, z)

	$\|z\|$	$\langle\|z\|\rangle$	V_θ	$M(R)$	$N(R)$	c_1/k_0^2	c_2/k_0^2	c_3/k_0^2	c_5/k_0^2
$R'=8$ 8.	>1 <1	1 60 0 45	135 205	934	4 36	0 16	8.4×10⁻³	20 0	0 19
$R_0=10$.	>1 <1	1 60 0 45	155 185	2260	12 0	0 16	8 4×10⁻³	18 8	0 08
Average						0 16	8 4×10⁻³	19 4	0 14

$L_0 \sim 0.4$, in which case we obtain the values of the c constants in units of k_0^2 given in Table 9. The average values of the constants at the bottom of Table 9 then lead to the equation

$$V_\theta = \frac{19.4R}{0.16 + 0.84(R/10)^2 + 0.14z^2}, \tag{17}$$

which approximates the observed variation of V_θ with R and z within the framework of the ellipsoidal hypothesis. Differentiation of equation (12) or (17) then gives the value of R for which V_θ is a maximum as a function of z,

$$R_{\max} = 10(0.19 + 0.17\, z^2)^{1/2} \tag{18}$$

and, by means of equations (8) and (9), the variation of A with z:

$$A = \frac{16}{1 + 0.14z^2}. \tag{19}$$

Equation (17) differs from those generally employed in the past in that it contains a z-term which is non-negligible for the Miras. It indicates that the value of V_θ for $z = 0$ (analogous to those derived from Cepheids or B stars) may be larger by as much as 5–10 km/sec than the value of V derived from equation (7) for a sample of stars for which $\langle|z|\rangle \geq 0.5$. The value of A must be corrected similarly according to equation (19).

Three comments should be made regarding the c constants used in equations (17), (18), and (19). First, the reliability of c_5, the coefficient of z^2, depends on a relatively small sample (53 stars) with $|z| > 1$, and it applies only to the short-period Miras. Our estimate of c_5 can and should be improved by more radial-velocity data for stars with large z-distances. Furthermore it would be of interest to make estimates of c_5 for the

© American Astronomical Society • Provided by the NASA Astrophysics Data System

1965ApJ...142..943S

Miras of longer period as well as those in the interval $140 < P < 240$. Second, the numerical value of the c constants are based on the value $L_0 = 0.4$ required by our rotation-curve for the group with $140 < P < 240$. This value of L_0 is smaller by a factor of 2 than that obtained directly from observation by Feast and by us. We interpret this discrepancy as follows: the value of V_θ at $R = R_0$ increases with period from about 180 km/sec at $P = 200$ days to about 240 km/sec at $P = 400$ days. In view of the period-frequency functions of other classes of kinematically homogeneous variable stars (e.g., the classical Cepheids or the RR Lyrae stars in a given globular cluster), it is reasonable to suppose that the Miras consist of a mixture of several or perhaps a continuum of kinematic families with overlapping period-frequency functions. If this be true, then σ_θ for any period interval will be overestimated because the peculiar motions upon which it is based are measured not relative to the true mean values of V_θ but rather they are measured relative to a value of V_θ that represents a weighted average over all the kinematic groups present in the period interval. Clearly, if our suppositions are correct, a criterion other than period or radial velocity is needed to make more meaningful subdivisions of the Miras for the analysis of their motions. Third, one may question whether the ellipsoidal hypothesis should be invoked at all in a discussion of kinematics over the range of distances involved in this study. It is particularly disturbing that the predicted value of $R_{\max} = 4.5$ for the $140 < P < 240$ group differs so greatly from the observed values of 8–9 kpc for the B stars (Münch and Münch 1964) and the 21-cm observations (Kwee, Muller, and Westerhout 1954). On the other hand, it must be noted that our observations do not allow $R_{\max}$ to be greater than 8 kpc (see Table 5). Clearly it will be preferable to construct an empirical distribution $V_\theta(R, z)$ upon which an improved theory can be based. This will require observation of many more distant variables. Such observations are within the grasp of existing telescopic facilities and are well worth pursuing.

Finally, it should be remarked that we have deliberately not chosen a value of a_0 on which to base final estimates of A or, more generally, the shapes of the galactic rotation-curves. In our opinion, the several difficulties mentioned in § VI*a* and in the preceding paragraph must *all* be confronted before a definitive description of the kinematics of the Miras can be constructed.

REFERENCES

Abt, H. A , and Golson, J. C. 1962, *Ap. J.*, **136**, 363.
Campbell, W. W., and Moore, J. H. 1918, *Pub. Lick Obs.*, **13**, 75.
Feast, M. 1963, *M N* , **125**, 367.
Johnson, H. L. 1965, *Ap. J.* (in press).
Joy, A H. 1947, *Ap. J.*, **106**, 288.
Kraft, R. P., and Schmidt, M. 1963, *Ap. J.*, **137**, 249.
Kwee, K. K., Muller, C. A., and Westerhout, G. 1954, *B.A.N.*, **12**, 220.
Merrill, P. W. 1923, *Ap. J.*, **58**, 195.
———. 1941, *ibid* , **94**, 171.
Merrill, P. W., and Wilson, R. E. 1942, *Ap. J.*, **95**, 248.
Münch, G , and Münch, L. 1964, *Ap. J.*, **140**, 162.
Oort, J. H. 1928, *B.A.N.*, **4**, 269.
Osvalds, V., and Risley, A. M. 1961, *Pub. Leander McCormick Obs.*, Vol. **11**, Part 21.
Parenago, P. 1945, *Astr. Zhur.*, **22**, 129
Rubin, V. C., and Burley, J. 1964, *A.J.*, **69**, 80.
Smak, J. I. 1964, *Ap. J. Suppl* , **9**, 141.
Stromberg, G. 1936, *Ap. J.*, **84**, 555.
Zonn, W. 1956, *Astr. Zhur.*, **33**, 855.

© American Astronomical Society • Provided by the NASA Astrophysics Data System